ITC 2/47

Journal of Information Technology and Control
Vol. 47 / No. 2 / 2018
pp. 209-219
DOI 10.5755/j01.itc.47.2.16670

Forward Adaptive Laplacian Source Coding Based on Restricted Quantization

Received 2016/11/04 | Accepted after revision 2018/03/05

http://dx.doi.org/10.5755/j01.itc.47.2.16670

Forward Adaptive Laplacian Source Coding Based on Restricted Quantization

Bojan Denic, Zoran Peric, Nikola Vucic
University of Nis, Faculty of Electronic Engineering, Department of Telecommunications,
Aleksandra Medvedeva 14, 18000 Nis, Serbia,
e-mail: bojan.denic@elfak.rs, zoran.peric@elfak.ni.ac.rs, vucicnikola90@gmail.com

Vladimir Despotovic
University of Belgrade, Technical Faculty in Bor Vojske Jugoslavije 12, 19210 Bor, Serbia,
e-mail: vdespotovic@tfbor.bg.ac.rs

Corresponding author: bojan.denic@elfak.rs

A novel solution for Laplacian source coding based on the three-level restricted quantization is proposed in this paper. The restricted quantization provides the reduction of granular distortion with the proper choice of the support region. We use the combination of two three-level restricted quantizers having unequal support regions, which are selected based on the lower distortion. The quantizers are designed using the Lloyd-Max's algorithm, by assuming the restricted Laplacian distribution of the input signal. The outputs are encoded using the Huffman code. In order to improve the performance the forward adaptive algorithm was employed, where the adaptation to the signal variance (power) was performed on frame-by-frame basis. Theoretical analysis has shown that in this manner the robustness and adaptability of the proposed solution is enabled. The experimental results prove that the proposed switched three-level restricted quantizer is superior in comparison to the three-level unrestricted quantizer, and outperforms the one-bit (two-level) Lloyd-Max's quantizer, while offering performance comparable to the two-bit (four-level) Lloyd-Max's baseline with large savings in bit rate.

KEYWORDS: Restricted scalar quantization, switched quantization, Lloyd-Max's algorithm, Huffman code, forward adaptation.

1. Introduction

Quantization is the most important step in analog-to-digital (A/D) signal conversion. It implies approximating a continuous range of values with a finite (preferably small) range of discrete values known as codewords. In an optimal quantizer design, the task is to design a quantizer, for the assumed probability density function (pdf) of the signal, such that the quantization error is minimal. While there is no restriction imposed on the chosen pdf, if it deviates from the one for which the optimal quantizer is designed for, the performance of the quantizer decreases.

Lloyd-Max's algorithm is extensively used in optimal scalar quantizer design (minimizes the mean squared error) [4, 10, 11, 20]. It iteratively computes the quantization parameters (representative levels and decision thresholds) starting from some initial values, and converging to the optimal ones in a finite number of steps [8]. It works fast when the number of levels N is low, but can be time-consuming for high N.

The asymptotic theory (high-resolution quantization) considers the issue of reduced complexity of design and implementation using the optimal companding quantization [4, 10, 11, 20], which has been widely applied in signal processing either for fixed length [16, 18, 19] or for variable length coding [6].

The quality of the quantized signal is influenced by the width of the quantizer's support region and if the input signal exceeds this support region, the clipping occurs, which introduces the error known as the overload distortion. If the quantizer's support region is decreased, the space between its output values (i.e. the granular region) is also decreased, leading to smaller granular distortion, but at the same time increasing the overload distortion. Hence, the quantizer design requires determining a balance between granular and overload distortion [13].

When the bounds of the support region are infinite, we consider the case of unrestricted quantizer. Restricting the bounds to finite values defines the restricted quantizer. The main idea behind the use of restricted instead of unrestricted quantization lies in the fact that it provides reduction of the granular distortion (improves the signal quality) with the decrease of the support region for a fixed number of quantization levels N (the levels density is increased). The proper choice of bounds for the support region is of extreme importance [13, 14].

Recently, restricted quantization was analyzed in [18] and [19]. Forward adaptive restricted and unrestricted scalar compandors with the same compression function and the same number of representative levels were introduced in [18] for Laplacian sources, where the restricted compandor was used whenever all the signal amplitudes within the frame were inside the support region, else the unrestricted one was used. In this way, the granular distortion was decreased, while the overload distortion was completely eliminated. A similar analysis for the Gaussian sources was conducted in [16].

The systems exploiting three-valued alphabet have been reported in [1, 2, 5, 21, 22]. In [1] and [2], it was applied in ECG compression and sensor network systems, respectively, while in [5], it was efficiently used in delta modulation system for Laplacian source coding. The steganography method known as LSB matching was studied in [21] and [22], where the three-valued alphabet has been added to the pixel values of the cover image.

In this paper, we developed the three-level quantizer with a goal to upgrade the one-bit quantizer solution. Note that the asymptotic theory does not apply here, since the optimal performance could not be achieved. It is designed employing the Lloyd-Max's algorithm, while its outputs are encoded using the Huffman code [7, 20]. We propose the use of switched quantization, choosing between two restricted quantizers with different support regions, unlike [16, 18, 19], where the combination of restricted and unrestricted quantizer was used. Moreover, we use a different switching rule, with minimal distortion being the criterion for switching.

The quantizers use the forward adaptation technique [11, 15, 17], which is an efficient way to improve the performance in terms of adaptability and robustness [3, 9]. Moreover, it gives better performance in the wide variance range of the input signal than the backward adaptation [17], and it is less sensitive to transmission errors [11]. However, unlike the backward adaptation, it requires the transmission of side information to the receiving part. In contrast to the solutions in [16] and [18] where the authors want to achieve the maximization in the signal quality, the proposed solution offers high data compression.

The performances of the proposed codec are evaluated using the Signal to Quantization Noise Ratio (SQNR) and bit rate. The effectiveness of the proposed algorithm has been proven theoretically and experimentally. The experimental results are compared with the baselines including three-level unrestricted quantization, one-bit and two-bit Lloyd-Max quantization [4, 10, 11, 20].

The reminder of the paper is organized as follows: in Section 2 we present a detailed description of design of the restricted three-level quantizer and the switched quantizer with the forward adaptive coding scheme. In Section 3 we present and discuss the experimental results and finally we give concluding remarks in Section 4.

2. Scalar Quantizer Design

2.1. Restricted Three-Level Scalar Quantizer

The restricted three-level scalar quantizer Q_R is specified by the parameters referred to as decision thresholds t_i such that $-t_{max} = t_0 < t_1 < t_2 < t_3 = t_{max}$, where t_{max} is the upper bound and $t_i \in R$, and representative levels $Y = \{y_1, y_2, y_3\} \subset R$, such that $y_1 < y_2 < y_3$, where $N = 3$ is a codebook size.

Quantization cells denoted with α_i are defined as $\alpha_i = (t_{i-1}, t_i]$, $i = 1, 2, 3$. Each cell α_i is represented by the level $y_i \in \alpha_i$. If the input signal value x falls into the interval α_i, that value is quantized by the level y_i. Therefore, a scalar quantizer can be defined as a function Q_R: $R \to Y$ that maps value x into level y_i where $Q_R(x) = y_i$, for $x \in \alpha_i$. The cells α_i constitute the granular region, hence the name granular cells.

In Figure 1, we present the symmetrical three-level quantizer involving zero level y_2. Due to the symmetry, the following equations will hold: $-t_1 = t_2$ and $-y_1 = y_3$. Therefore, the design of the proposed quantizer includes finding the parameters t_2 and y_3 for a given t_{max}.

Figure 1

The proposed restricted three-level quantizer

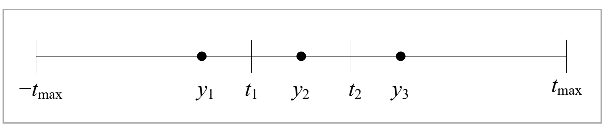

We presume that information source that needs to be quantized is memoryless and zero-mean restricted Laplacian with probability density function (pdf) [4, 10, 11, 20]:

$$p(x,\sigma) = \frac{1}{\sqrt{2}\sigma} \frac{\exp\left(-\frac{\sqrt{2}|x|}{\sigma}\right)}{\left(1-\exp\left(-\frac{\sqrt{2}t_{max}}{\sigma}\right)\right)} \tag{1}$$

where σ is the standard deviation.

Lloyd-Max's algorithm was applied in the following steps:

Step1. Initialization of the threshold $t_2^{(0)} = 0.71\sigma_{ref}$ and level $y_3^{(0)} = 1.42\sigma_{ref}$ [5].

Step2. Computation of new values of level y_3 and threshold t_2 using [11]:

$$y_3^{(i+1)} = \frac{\int_{t_2^{(i)}}^{t_{max}} x p\left(x,\sigma_{ref}\right) dx}{\int_{t_2^{(i)}}^{t_{max}} p\left(x,\sigma_{ref}\right) dx}, \quad i = 1,2,... \tag{2}$$

$$t_2^{(i+1)} = \frac{y_2^{(i+1)} + y_3^{(i+1)}}{2}, \quad i = 1,2,... \tag{3}$$

Step3. Interruption of the Lloyd-Max's algorithm when next iteration does not produce any change in distortion.

The mean squared distortion D, which is used as a measure of the error introduced by the restricted quantizer, is given by [4, 10, 11, 20]:

$$D(\sigma) = 2\int_0^{t_2} x^2 p(x,\sigma) dx + 2\int_{t_2}^{t_{max}} (x-y_3)^2 p(x,\sigma) dx. \tag{4}$$

SQNR, which is used as a measure of the quality of the quantized signal, is given by [4, 10, 11, 20]:

$$\mathrm{SQNR}(\sigma) = 10\log_{10}\left(\frac{P_{sor}(\sigma)}{D(\sigma)}\right), \tag{5}$$

where $P_{sor}(\sigma)$ is the power of the input source defined as [11]:

$$P_{sor}(\sigma) = 2\int_{0}^{t_{\max}} x^2 p(x,\sigma)\,dx\,. \tag{6}$$

Let p_1, p_2 and p_3 denote probabilities that a sample of the input signal belongs to the first, second or third quantization cell, respectively:

$$p_3(\sigma) = p_1(\sigma) = \int_{t_2}^{t_{\max}} p(x,\sigma)\,dx = \frac{1}{2} - \frac{\exp\left(-\frac{\sqrt{2}t_2}{\sigma}\right) - 1}{2\left(\exp\left(-\frac{\sqrt{2}t_{\max}}{\sigma}\right) - 1\right)}, \tag{7}$$

$$p_2(\sigma) = 2\int_{0}^{t_2} p(x,\sigma)\,dx = \frac{\exp\left(-\frac{\sqrt{2}t_2}{\sigma}\right) - 1}{\exp\left(-\frac{\sqrt{2}t_{\max}}{\sigma}\right) - 1}. \tag{8}$$

The quantizer representative levels are encoded using the Huffman code. The level having the highest probability is encoded with codeword '**0**' and the other two levels are encoded with the codewords '**10**' and '**11**'.

The bit rate is defined as [20]:

$$R(\sigma) = \sum_{i=1}^{N=3} p_i(\sigma) l_i\ , \tag{9}$$

where l_i is the length of the Huffman codeword corresponding to the level y_i.

In Figure 2, we illustrate the dependence of SQNR of the restricted quantizer Q_R, which is designed for different values of the support region upper bound $t_{\max}$ (using Lloyd-Max's algorithm) and $\sigma = \sigma_{\mathrm{ref}} = 1$. We observe the gain in performance in terms of SQNR compared to the unrestricted quantizer Q_{UR} ($t_{\max} \to \infty$) [5], especially when Q_{UR} is designed for smaller $t_{\max}$ values. Note that designing for larger $t_{\max}$ (e.g. for $6\sigma_{\mathrm{ref}}$) provides the SQNR score close to the one of Q_{UR}.

Figure 2

SQNR dependence on the upper bound threshold t_{max} for the proposed three-level restricted quantizer

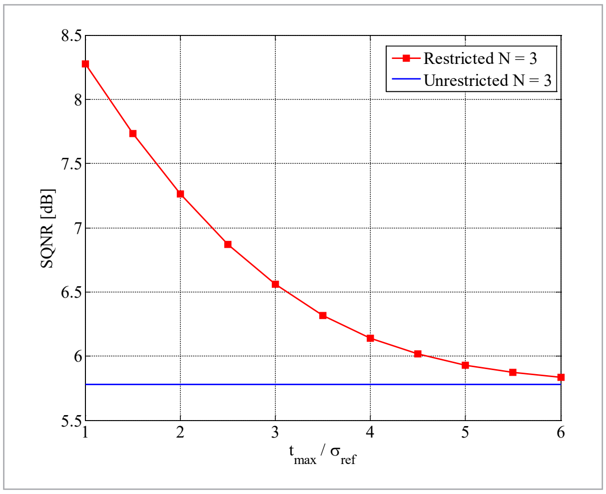

The dependence of the probability that a sample of the input signal belongs to a particular quantization cell on $t_{\max}$ is depicted in Figure 3, demonstrating that p_2 representing the cell $\alpha_2 = (-t_2, t_2)$ is more probable than the other two. The probability p_2 increases for higher $t_{\max}$.

Figure 3

Probabilities p_1 and p_2 for the restricted three-level quantizer

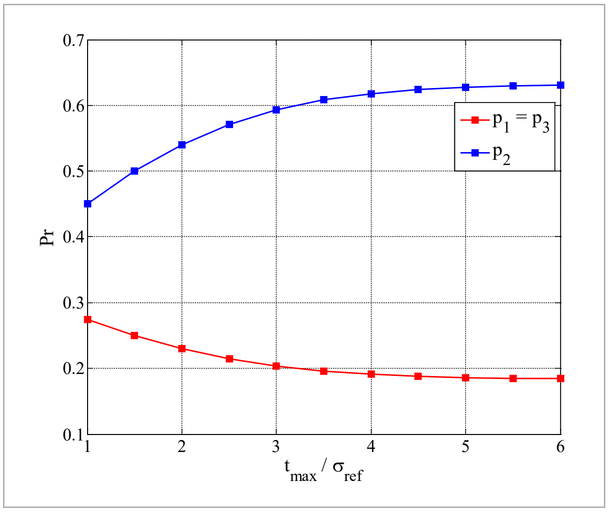

We can guarantee that the restricted quantization is a suitable solution for the sources bounded by the amplitude, but the situation changes when we deal with the unrestricted ones. This effect is visible in Figure 4, where the higher probability that the sample occurs outside the restricted quantizer support region indicates the higher amplitude mismatch (between the designed range of the quantizer and the input infinite range), leading to larger quantization error.

In order to eliminate this drawback, we propose the switched quantization that will be described in the next subsection.

Figure 4

The probability of sample occurrence outside the restricted quantizer support region

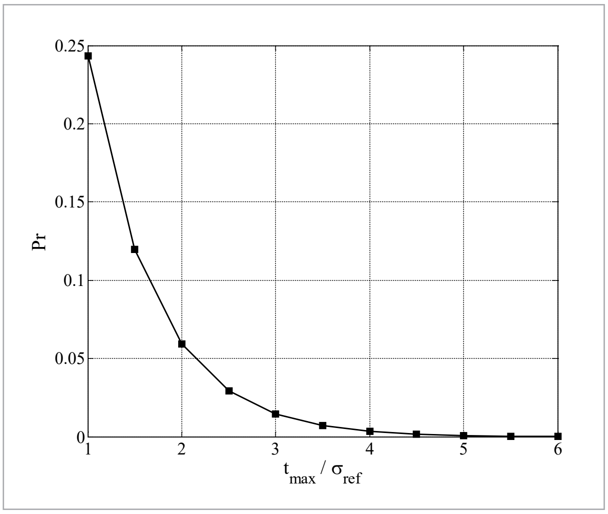

2.2. Switched Quantization

In this subsection, we propose a model of switched quantizer (denoted by Q_s) that instead of just one employs two restricted three-level quantizers. Let $t_{\max1}$ and $t_{\max2} = t_{\max1} + \Delta$ be the upper bounds of the three-level restricted quantizers having smaller (Q_{R1}) and wider support region (Q_{R2}), respectively. Note that Δ should be determined such that all amplitudes of the input signal outside the support region of Q_{R1} belong to the support region of Q_{R2}. Ideally, the upper bound of $t_{\max2}$ should be $t_{\max2} \to \infty$ [5] and in that case Q_s provides amplitude matching for any source. However, we distinct from that scenario and design Q_{R2} with limited upper bound, in order to exploit the benefit in SQNR that offers restricted quantization compared to the unrestricted one (see Figure 2). Figure 4 shows that $t_{\max2} \geq 3\sigma_{\mathrm{ref}}$ is a reasonable choice of the upper bound. Moreover, it can be shown that for Laplacian pdf, 98.6% of all samples lay in the interval ($-3\sigma_{\mathrm{ref}}$, $3\sigma_{\mathrm{ref}}$). The following switching rule is implemented to select the desired quantizer: the switched quantizer uses Q_{R1} if it produces smaller value of distortion than Q_{R2}.

The total distortion D_t introduced by the proposed switched quantizer can be expressed as [18]:

$$D_t(\sigma) = wD_1(\sigma) + (1-w)D_2(\sigma), \tag{10}$$

where $D_1(\sigma)$ and $D_2(\sigma)$ are given by (4) and denote distortions inserted by Q_{R1} and Q_{R2}, respectively, while w is the weight that determines the proportion of Q_{R1}.

Signal to quantization noise ratio in this case can be determined as [11]:

$$\mathrm{SQNR}_s(\sigma) = 10\log_{10}\left(\frac{\sigma^2}{D_t(\sigma)}\right). \tag{11}$$

The bit rate of the switched quantizer can be calculated as:

$$R_s(\sigma) = wR_1(\sigma) + (1-w)R_2(\sigma). \tag{12}$$

where R_1 and R_2 are given by (9) and represent bit rates of Q_{R1} and Q_{R2}, respectively.

Figure 5

SQNR vs. R for the Lloyd-Max quantizers

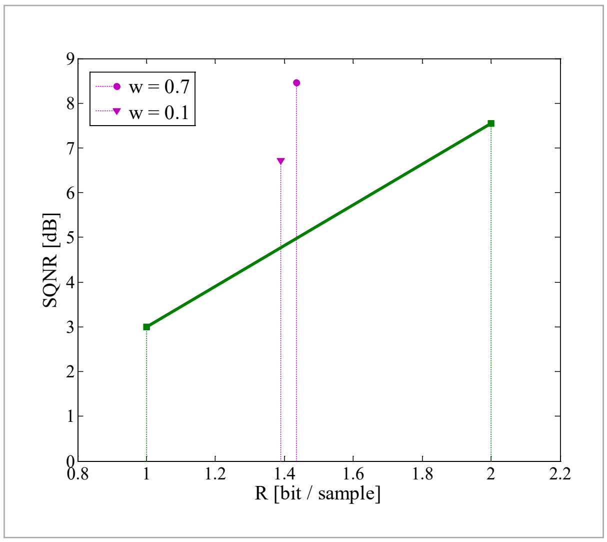

Let us consider the special case of Q_s when it combines Q_{R1} ($t_{\max 1} = 2\sigma_{\text{ref}}$) and Q_{R2} ($t_{\max 2} = 4\sigma_{\text{ref}}$), where w is assumed to be 0.1 and 0.7. To determine the potential benefit of the given Q_s, we use as baselines one-bit and two-bit Lloyd-Max's quantizer [11, 20], since the number of quantization levels of the proposed quantizer is in-between the two baselines. The achieved performance is shown in Figure 5. It can be seen that it provides 3.48 dB (w = 0.7) and 1.95 dB (w = 0.1) higher SQNR value compared to the one (specified by a point on a curve) attained by the baseline quantizer having the same bit rate. Observe that SQNR increases by more frequent selection of Q_{R1} (w = 0.7).

2.3. Forward Adaptive Quantization

Both restricted quantizers used in the switched quantization scheme described in Section 2.2 are realized using the forward adaptive technique, as shown in Figure 6. It consists of a buffer, a variance estimator, an L-levels log-uniform quantizer Q_{LU} and an encoder with two adaptive restricted quantizers (Q_{R1} and Q_{R2}). The output of the restricted quantizer is encoded using the Huffman code. The quantizers are adapted to the short-term estimate of the variance (power) for each frame of the input signal. Therefore, it is necessary to adjust the quantizer's codebook framewise. The following procedure is performed.

Figure 6

Forward adaptive coding scheme: (a) encoder, (b) decoder

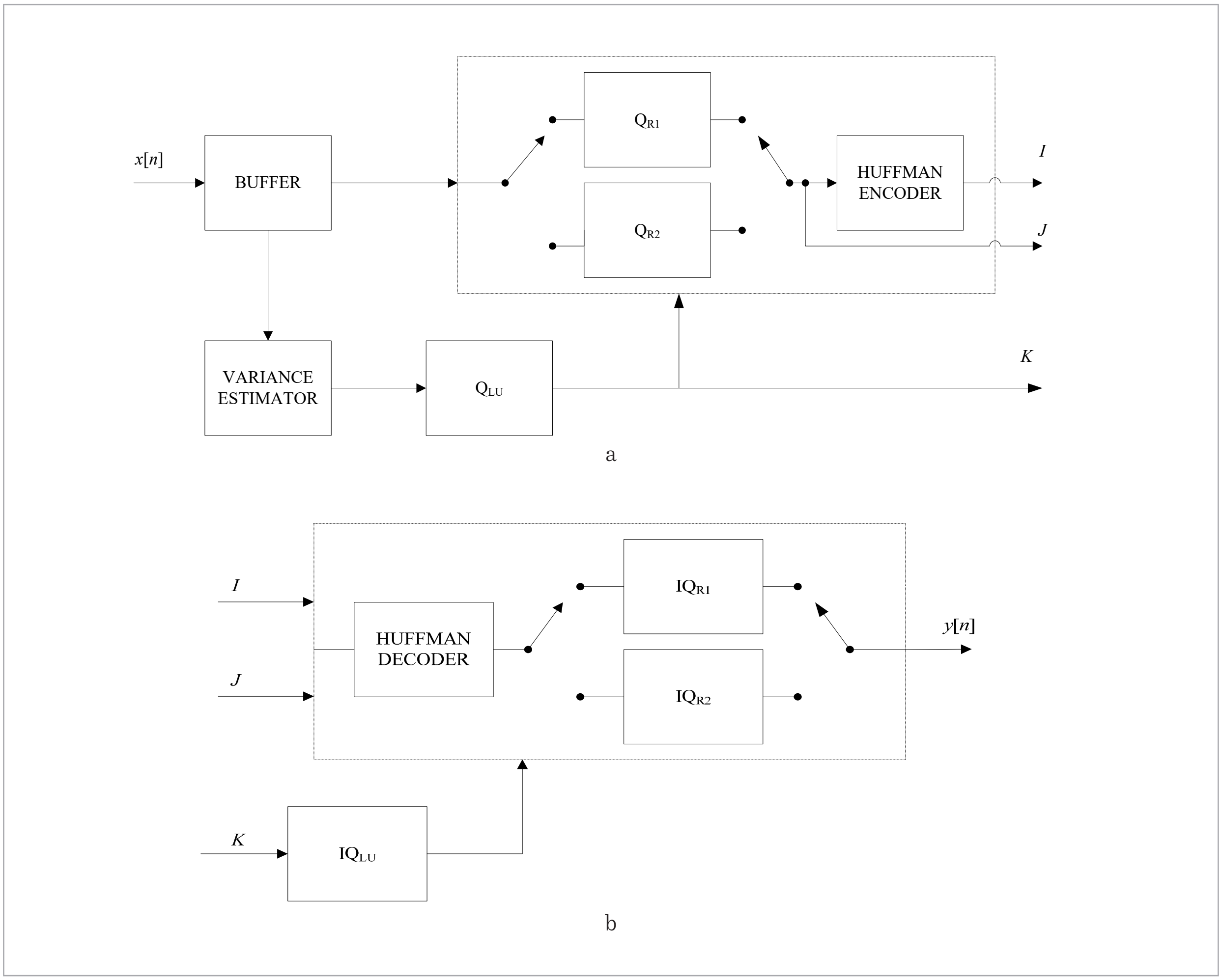

Buffer is used for storage of frame with M samples. The samples within the buffer are denoted as x_i, i = 1, 2,..., M. The variance estimator calculates the variance σ^2 within one frame. It is used for adaptation and has to be quantized since the information about it has to be available at the decoder side.

For the variance quantization, we have used a log-uniform scalar quantizer (Q_{LU}), since it attains better performance (more constant SQNR in a wide dynamic range) compared to the uniform one [15]. Particularly, the log-uniform quantizer having L levels is designed for quantizing the logarithmic variance α[dB] = $10\log_{10}(\sigma^2/\sigma_0^2)$ in the range (-30dB, 30dB) with respect to referent variance (power) σ_0^2.

The thresholds and levels in the logaritmic domain are given by (13) and (14), respectively:

$$l_i[\text{dB}] = -30 + i\Delta_L\ ,\ i = 0,\ldots,L\ , \tag{13}$$

$$\hat{l}_i[\text{dB}] = -30 + \left(i - \frac{1}{2}\right)\Delta_L\ ,\ i = 1,\ldots,L\ , \tag{14}$$

where $\Delta_L = 60/L$ [dB] is the step size.

In the linear domain, they are given by (15) and (16), respectively:

$$r_i = \sigma_0^2 10^{l_i/10}\ ,\ i = 0,\ldots,L\ , \tag{15}$$

$$\hat{r}_i = \sigma_0^2 10^{\hat{l}_i/10}\ ,\ i = 1,\ldots,L\ . \tag{16}$$

The quantization rule is given by $Q_{LU}(\sigma^2) = \hat{r}_i$ for $\sigma^2 \in (r_{i-1}, r_i)$.

The parameters of the k-th adaptive quantizer, k = 1, 2, are updated according to the quantized value of the frame variance, and for $\sigma^2 \in (r_{i-1}, r_i)$, they can be respectively determined as: $t_{\max,k}{}^a = g_i \cdot t_{\max,k}(\sigma_{\text{ref}})$, $t_{2,k}{}^a = g_i \cdot t_{2,k}(\sigma_{\text{ref}})$, $y_{3,k}{}^a = g_i \cdot y_{3,k}(\sigma_{\text{ref}})$, where $g_i = \sqrt{\hat{r}_i}$. These parameters are constant inside the current frame. With $t_{\max,k}(\sigma_{\text{ref}})$, $t_{2,k}(\sigma_{\text{ref}})$ and $y_{3,k}(\sigma_{\text{ref}})$ we denote maximal amplitude, threshold and level of the non-adaptive (designed for σ_{ref}) restricted quantizer, respectively.

Quantization for the particular frame is performed using both quantizers and distortions are estimated. The encoder makes a selection of the quantizer based on lower distortion.

Indices I, J and K in Figure 6a are transmitted to the receiver. Index I carries the information about the encoded signal samples, while index J denotes the selected restricted quantizer and it is encoded with one-bit codeword '**0**' or '**1**'. Information about the quantized variance used for adaptation is transmitted with index K using the fixed length codewords of $\log_2 L$ bits. J and K are transmitted as side information for each frame.

Decoder is shown in Figure 6b. It consists of inverse encoder with two inverse restricted quantizers Q_{R1} and Q_{R2}, and inverse log-uniform quantizer Q_{LU}. Based on index J, the encoder determines which quantizer is used for the current frame. Using index K, side information is decoded and parameters of the inverse quantizer are adapted. Using index I, the decoded samples in the current frame are reconstructed.

Figure 7 shows the theoretical results in the entire input variance range of interest for SQNR of the forward adaptive quantizer Q_R with two different upper bounds and the switched quantizer Q_s that combines these quantizers (w = 0.7). The results are obtained according to (5) for Q_R and (11) for Q_s, for L=32 levels log-uniform quantizer and $\sigma_0^2 = 2 \times 10^{-3}$. In Figure 8, we illustrate the dependence of bit rate of the Q_s in the same range of variance, using (12).

Note that SQNR(α) and $R(\alpha)$ are periodic functions,

Figure 7

Theoretical results: SQNR in a wide dynamic range of input variance for L = 32 levels log-uniform quantizer

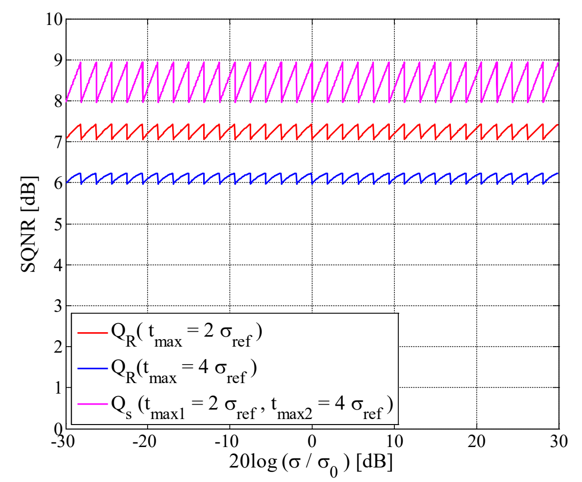

Figure 8

Theoretical results: Bit rate R of the switched quantizer versus the input variance for L = 32 levels log-uniform quantizer

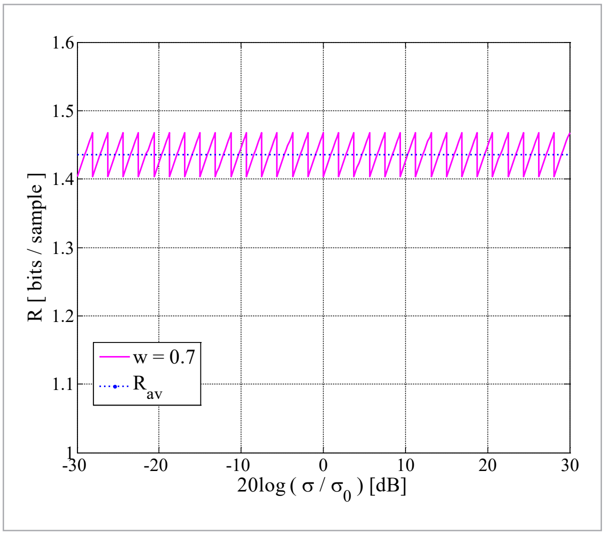

and the number of periods corresponds to the number of levels of the log-uniform quantizer.

In order to obtain the average values of these functions inside one period (α_1, α_2), we use the following expressions [18]:

$$\mathrm{SQNR}_{s,av} = \frac{1}{(\alpha_2 - \alpha_1)} \int_{\alpha_1}^{\alpha_2} \mathrm{SQNR}_s(\alpha) d\alpha, \tag{17}$$

$$R_{s,av} = \frac{1}{(\sigma_2 - \sigma_1)} \int_{\sigma_1}^{\sigma_2} R_s(\sigma) d\sigma, \tag{18}$$

where $\sigma_1 = \sigma_0 10^{\alpha_1/20}$ and $\sigma_2 = \sigma_0 10^{\alpha_2/20}$.

Based on Figures 7 and 8, we observe that the average values of $\mathrm{SQNR}_{s,av}$ and $R_{s,av}$ obtained for the switched quantizer Q_s comply with the results presented in Figure 5.

Now, we can define the average bit rate for the adaptive switched quantizer as:

$$R_{s,av}^{a} = R_{s,av} + \frac{\log_2 L + 1}{M}, \tag{19}$$

where the second term is the side information.

3. Experimental Results and Discussion

The performance of the proposed codec is tested for speech signal, as it was shown that Laplacian pdf accurately models speech for frames shorter than 200 ms [12]. Moreover, the speech is an example where the small amplitude values are more likely than large ones, which is beneficial since we deal with restricted quantization.

Training sequence of approximately one million speech samples (Serbian language, male speaker, sampled at 16 kHz) was used to determine the weight w, which denotes the proportion of Q_{R1} (see Section 2.2). The proposed codec was then applied to test speech signal that was not included in the training sequence. This test speech contains 66 500 samples spoken in Serbian language and sampled at 16 kHz.

As an objective measure of quality the segmental SQNR is used [4, 10, 11, 20], which is calculated separately over all speech frames and then averaged. It was observed that classical SQNR is not a good measure of speech quality as it averages the ratio over the entire signal, which is not stationary. Speech energy fluctuates over time, hence parts of signal where energy is large should not dominate the noisy parts where speech energy is small, or vice versa. Segmental SQNR better matches the perceptual speech quality, i.e. frames with large speech energy do not dominate the overall perceptual quality, since the existence of noisy frames drives the overall quality lower.

Finally, the segmental signal to quantization noise ratio (SQNR) for the switched model of quantizer has the form:

$$\mathrm{SQNR}_{\mathrm{seg}} = w\mathrm{SQNR}_{\mathrm{seg},1} + (1-w)\mathrm{SQNR}_{\mathrm{seg},2}, \tag{20}$$

where w is the share of the frames processed with the restricted quantizer Q_{R1}, $\mathrm{SQNR}_{\mathrm{seg},1}$ is SQNR for frames processed with Q_{R1} and $\mathrm{SQNR}_{\mathrm{seg},2}$ is SQNR for frames processed with Q_{R2}.

Figure 9 presents the share of frames processed with the restricted quantizer Q_{R1} obtained on the training sequence for different frame sizes. Note that w slightly decreases as the frame size increases, i.e. the quantizer Q_{R1} with smaller support region is used less often for longer frames.

Figure 9

Proportion of frames processed with the restricted quantizer Q_{R1} depending on the frame size

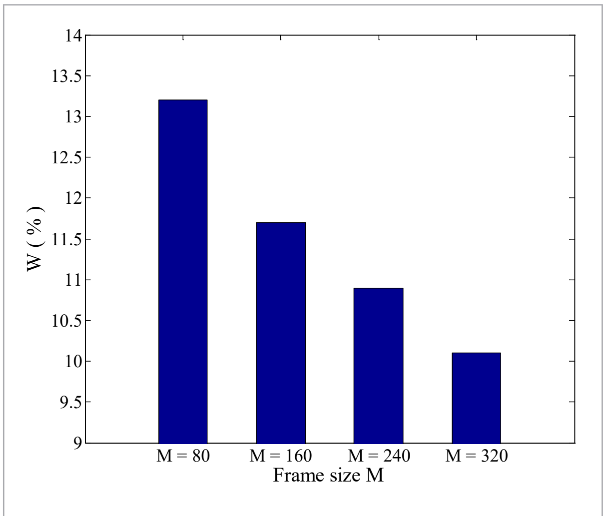

Figure 10

The distribution of the quantizer's upper support bound normalized by the standard deviation (t_{max}/σ) over signal frames (M = 320)

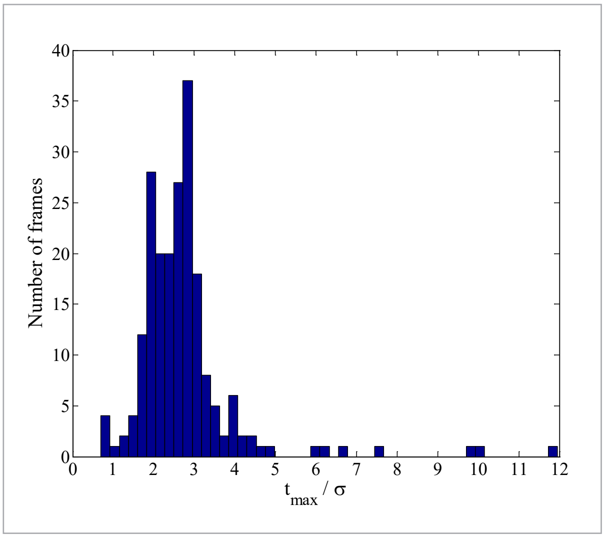

The set of restricted quantizers is designed in the range $t_{max} \in (\sigma_{ref}, 6\sigma_{ref})$, and the performance of the switched quantization scheme that combines the two quantizers (Q_{R1} and Q_{R2}) from a given set is evaluated for test speech signal. The performed experiment reveals that the proposed coding algorithm with Q_s achieves the highest segmental SQNR value when the non-adaptive quantizer parameters are chosen as follows, Q_{R1}: $t_{max1} = 1.1\sigma_{ref}$ and Q_{R2}: $t_{max2} = 3\sigma_{ref}$.

Indeed, if we observe in Figure 10 the distribution of the upper support bound determined over all speech signal frames and normalized by the standard deviation for the particular frame (t_{max}/σ), we see that the majority of frames have $1.1 \le t_{max}/\sigma \le 3$, with most of the frames having $t_{max}/\sigma = 3$. This justifies the choice of the upper support bounds for Q_{R1} and Q_{R2}.

In Figure 11, we present the signal to quantization noise ratio accross all signal frames (M = 320) for configuration with the switched Q_s and unrestricted three-level quantizer Q_{UR}. It can be seen that, both in active and in inactive speech frames, higher values of the SQNR are obtained for the switched restricted compared to the unrestricted quantizer.

Table 1 summarizes the performance measured by segmental SQNR and bit rate, for different frame sizes (M = 80, 160, 240 and 320 samples). The unrestricted three-level quantizer Q_{UR}, the two-level Lloyd-Max $Q_{N=2}$ and the four-level Lloyd-Max quantizer $Q_{N=4}$ are used as baselines. Based on the results in Table 1, one

Figure 11

SQNR across the frames of length M = 320, for the forward adaptive Q_s ($t_{max1} = 1.1\sigma_{ref}$ and $t_{max2} = 3\sigma_{ref}$) and Q_{UR} for L = 32 levels Q_{LU}

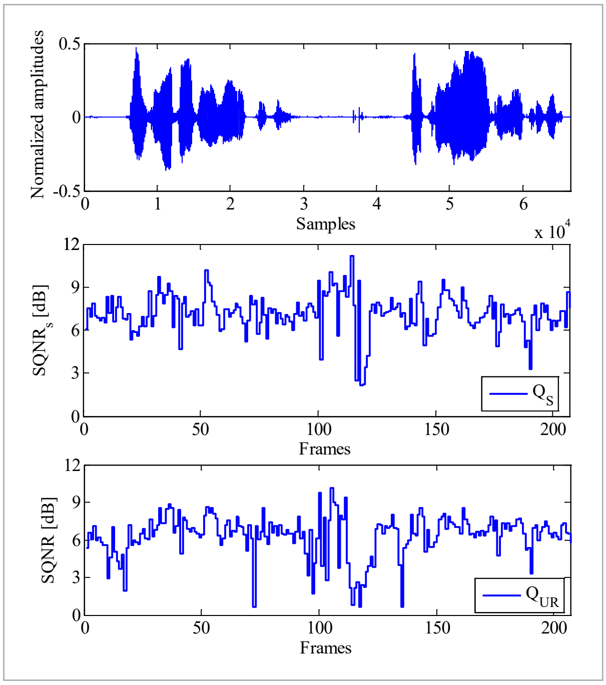

Table 1

Experimental results of different quantizers applied in the configuration in Figure 6, for various frame lengths

	$Q_S(t_{max1}=1.1\sigma_{ref}, t_{max2}=3\sigma_{ref})$		$Q_{UR}(t_{max} \to \infty)$		$Q_{N=2}$		$Q_{N=4}$	
	$SQNR_{seg}$ [dB]	R^a [b/s]	$SQNR_{seg}$ [dB]	R^a [b/s]	$SQNR_{seg}$ [dB]	R^a [b/s]	$SQNR_{seg}$ [dB]	R^a [b/s]
M=80	7.856	1.500	6.417	1.429	4.597	1.062	7.857	2.062
M=160	7.465	1.459	6.279	1.398	4.385	1.031	7.872	2.031
M=240	7.309	1.446	6.389	1.387	4.318	1.021	7.972	2.021
M=320	7.167	1.439	6.346	1.382	4.227	1.016	7.928	2.016

can perceive that the proposed switched quantizer Q_s attains the highest segmental SQNR at the frame length of $M = 80$ samples. Notice in that case that it offers SQNR comparable to $Q_{N=4}$, with reduction in bit rate of 0.562 bit/sample, while outperforming configuration with $Q_{N=2}$ by 3.26 dB with only 0.438 bit/sample higher bit rate.

The gain over Q_{UR} is approximatelly 1.43 dB, indicating the superiority of the proposed switched restricted quantizer over Q_{UR}.

Let us emphasize that the complexity of the proposed algorithm remains unchanged compared to the baselines, equal to $O(n^2)$, where n is the size of the input data set.

Figure 12

Theoretical results for Q_s: SQNR in a wide dynamic range of the input signal variance and for L = 32-levels Q_{LU}

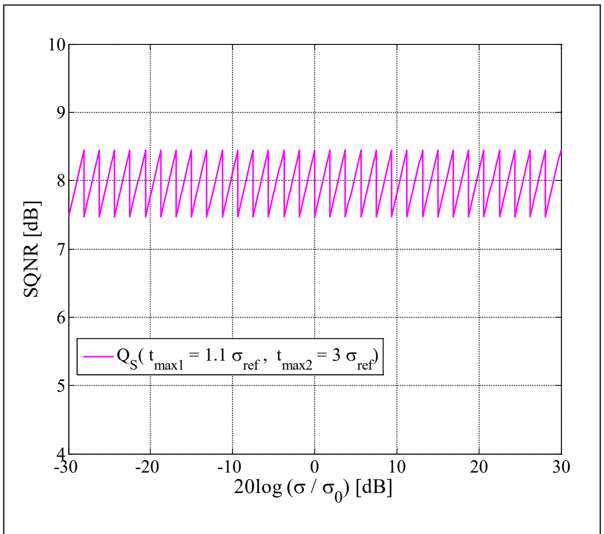

Note that the theoretical results shown in Figure 12 with the same parameters ($w = 0.132$, $t_{max1} = 1.1\sigma_{ref}$, $t_{max2} = 3\sigma_{ref}$) as in Table 1 are in agreement with the experimental ones ($M = 80$).

4. Conclusion

The switched restricted three-level quantization employing Huffman coding and its implementation to the forward adaptive algorithm was proposed in this paper. The algorithm performs frame-by-frame processing of the input signal, and the appropriate quantizer for each signal frame is chosen according to the criterion of lower distortion. Segmental SQNR and bit rate are used as a measure of performance. It was proved theoretically that the proposed algorithm offers high performance in terms of adaptability and robustness. The real speech signal was used to determine the upper bound thresholds of the involved restricted quantizers, while the effectiveness of the proposed algorithm was proven in comparison to three baselines: the three-level unrestricted quantizer and the Lloyd-Max quantizers with $N = 2$ and $N = 4$ levels.

The experimental results have shown that the proposed solution provides SQNR performance comparable to the $N = 4$ levels Lloyd-Max's baseline, with savings in bit rate of 0.562 bits/sample, while it significantly outperforms other observed quantizers.

Acknowledgments

This work was partly funded by the Ministry of Education and Science of the Republic of Serbia, grant no. TR32035 and TR32051, within the Technological Development Program.

References

1. Azarbad, M., Ebrahimzadeh, A. ECG Compression Using the Three-Level Quantization and Wavelet Transform. International Journal of Computer Applications, 2012, 59(1), 28–38. https://doi.org/10.5120/9515-3916
2. Canudas De Wit, C., Jaglin, J., Siclet, C. Energy-Aware 3-Level Coding and Control Co-Design for Sensor Network Systems. In: Proceedings of 16th IEEE International Conference on Control Applications, Singapour, Singapore, 2007.
3. Chen, Y., Hao, C., Wu, W., Wu, E. Robust Dense Reconstruction by Range Merging Based on Confidence Estimation. SCIENCE CHINA Information Sciences, 2016, 59:092103. https://doi.org/10.1007/s11432-015-0957-4
4. Chu, C. Speech Coding Algorithms. John Wiley & Sons, New Jersey, 2005.
5. Denic, B., Peric, Z., Despotovic, V. Three-Level Delta Modulation for Laplacian Source Coding. Advances in Electrical and Computer Engineering, 2017, 17(1), 95-102. https://doi.org/10.4316/AECE.2017.01014
6. Dincic, M., Peric, Z., Lukic, J., Denic, D. Designing of the Forward Adaptive Companding Quantizer with Variable Length Codewords for stochastic Measurement Signals. FACTA UNIVERSITATIS, Series: Electronics and Energetics, 2013, 26(2), 99-105.
7. Firmansah, L., Setiawan, E. B. Data Audio Compression Lossless FLAC Format to Lossy Audio MP3 Format with Huffman Shift Coding Algorithm. In: Proceedings of 4th IEEE International Conference on Information and Communication Technology (ICoICT), Bandung, Indonesia, 2016. https://doi.org/10.1109/ICoICT.2016.7571951
8. Gu, B., Sheng, V. S., Tay, K. Y., Romano, W., Li, S. Incremental Support Vector Learning for Ordinal Regression. IEEE Transactions on Neural Networks and Learning Systems, 2015, 26(7), 1403-1416. https://doi.org/10.1109/TNNLS.2014.2342533
9. Gu, B., Sheng, V. A Robust Regularization Path Algorithm for ν-Support Vector Classification. IEEE Transactions on Neural Networks and Learning Systems, 2016, 28(7), 1241-1248. https://doi.org/10.1109/TNNLS.2016.2527796
10. Hanzo, L., Somerville, C., Woodard, J. Voice and Audio Compression for Wireless Communications. John Wiley & Sons, London, 2007. https://doi.org/10.1002/9780470516034
11. Jayant, N. S., Noll, P. Digital Coding of Waveforms: Principles and Applications to Speech and Video. Prentice Hall, New Jersey, 1984.
12. Jensen, J., Batina, I., Hendriks, R. C., Heusdens, R. A Study of the Distribution of Time-Domain Speech Samples and Discrete Fourier Coefficients. In: Proceedings of IEEE First BENELUX/DSP Valley Signal Processing Symposium, 2005.
13. Na, S. On the Support of Fixed-Rate Minimum Mean-Squared Error Scalar Quantizers for a Laplacian Source. IEEE Transactions on Information Theory, 2004, 50(5), 937-944. https://doi.org/10.1109/TIT.2004.826686
14. Na, S., Neuhoff, D. L. On the Support of MSE-Optimal, Fixed-Rate, Scalar Quantizers. IEEE Transactions on Information Theory, 2001, 47(7), 2972-2982. https://doi.org/10.1109/18.959274
15. Nikolic, J., Peric, Z. Lloyd-Max's Algorithm Implementation in Speech Coding Algorithm Based on Forward Adaptive Technique. Informatica, 2008, 19(2), 255-270.
16. Nikolic, J., Peric, Z., Jovanovic, A. Two Forward Adaptive Dual-Mode Companding Scalar Quantizers for Gaussian Source. Signal Processing, 2016, 120, 129-140. https://doi.org/10.1016/j.sigpro.2015.08.016
17. Ortega, A., Vetterli, M. Adaptive Scalar Quantization Without Side Information. IEEE Transactions on Image Processing, 1997, 6(5), 665-676. https://doi.org/10.1109/83.568924
18. Peric, Z., Nikolic, J. An Adaptive Waveform Coding Algorithm and Its Application in Speech Coding. Digital Signal Processing, 2012, 22(1), 199-209. https://doi.org/10.1016/j.dsp.2011.09.001
19. Peric, Z., Nikolic, J., Mosic, A., Panic, S. A Switched-Adaptive Quantization Technique Using μ-Law Quantizers. Information Technology and Control, 2010, 39(4), 317–320.
20. Sayood, K. Introduction to Data Compression. Elsevier Science, San Francisco, 2005.
21. Xia, Z., Wang, X., Sun, X., Wang, B. Steganalysis of Least Significant Bit Matching Using Multi-Order Differences. Security and Communication Networks, 2014, 7(8), 1283-1291. https://doi.org/10.1002/sec.864
22. Xia, Z., Wang, X., Sun, X., Liu, Q., Xiong, N. Steganalysis of LSB Matching Using Differences Between Nonadjacent Pixels. Multimedia Tools and Applications, 2016, 75(4), 1947-1962. https://doi.org/10.1007/s11042-014-2381-8